Sequencing waves in single-transducer acoustophoretic patterning of microspheres

Sequencing Waves In Single-Transducer Acoustophoretic Patterning of Microspheres

Y. J. Wang,[1] L. A. Chai,[1] R. E. Zubajlo,[1] and B. W. Anthony[1, a)]
Department of Mechanical Engineering, Massachusetts Institute of Technology, Cambridge, MA 02139 USA

(Dated: 30 November 2022)

Acoustophoretic assembly uses acoustic waves to move dispersed particles into a geometric pattern. The pattern is typically created in a single step and often relies on wave-forming techniques to achieve the desired pattern geometries. We show that multiple acoustic waves can be applied sequentially in a multi-step process to create particle patterns not achievable by the individual waves alone. We demonstrate this approach in spherical particles using two planar pseudo-standing waves. Applied individually, each of the two waves would create linear particle bands with uniform spacing in between the bands. However, when applied sequentially, the banding pattern created in the first step is further manipulated by the second wave to create non-uniform spacing in between the bands. The experimentally achieved particle pattern geometry agrees well with the theoretical prediction.

[a)] Author to whom correspondence should be addressed: banthony@mit.edu

Arranging particles into user-defined patterns has a wide-range of applications, including fabricating functional biological tissue[5,16], organizing filler materials in composites[2,18,19,28,35], and creating crystalline and quasicrystal metamaterials[3,15]. The patterns can be formed by designing particles that interact with each other and self-assemble into the desired geometry or by applying an external force to move the particles into the desired geometry[14,21,33]. While electric[1,4], magnetic[26,29], and acoustic[9,27] fields have all been utilized to provide the external force, using electric and magnetic fields are limited to materials with specific electrical and magnetic properties. In contrast, using acoustic fields does not have such restrictions and is applicable to a wider range of materials[7].

The basic acoustophoretic patterning setup uses a single transducer to create a resonant pseudo-standing waves within the patterning chamber. The resulting acoustic radiation force (ARF) moves the particles either to the pressure nodes or antinodes of the wave, depending on the material properties. Thus, the particle pattern geometries that can be achieved with a single-transducer setup are typically limited to simple periodic patterns where groups of particles are spaced a half-wavelength apart. This limitation can be overcome by adding more transducers[3,15], ultrasonic arrays[12,13], acoustic holograms[22,23], and other wave-forming techniques[30] to control the acoustic pressure field. Wave-forming techniques have made it possible to create arbitrary particle pattern geometries in 2D and 3D[6,17,25]. However, these approaches may not be suitable for all applications. Space and cost constraints for applications such as extrusions for fiber manufacturing and 3D printing can make incorporating the hardware associated with wave-forming techniques challenging[20,24]. Thus, there remains a need to expand the pattern geometries that can be created with limited hardware. To address this need, we propose applying acoustic waves in sequence so that the particle pattern geometry created by one wave serves as the starting point of patterning by the next wave. This approach allows additional pattern geometries to be created from a small set of waves, which can expand the patterning capabilities of setups without needing to increase the number of transducers or adding other wave-forming capabilities. The goal of this paper is to provide a proof of concept demonstration that applying two waves in sequence can result in particle patterns not achievable with either wave alone. We show this is possible for microspheres in planar waves in a single-transducer setup.

The key principles for manipulating the pattern created by one wave with a second wave is that the ARF drives particles to their closest stable equilibrium locations and that particles do

not cross equilibrium locations. This means that each stable equilibrium location has an associated assembly zone, determined by the positions of the neighboring equilibrium locations. Particles that are located within the assembly zone of an equilibrium location when the acoustic field is initially applied will collect at that equilibrium location. Particles initially outside the assembly zone will collect at other equilibrium locations. If the acoustic field is applied when the particles are fully dispersed within the fluid medium, every stable equilibrium location will contain particles in the acoustophoretic pattern. However, if particles are evacuated from some assembly zones before the acoustic wave is applied, that equilibrium location will be left empty in the acoustophoretic pattern. Thus, the ability to selectively remove particles from certain regions of the device before applying the acoustic wave gives additional control to creating particle patterns. In our approach to acoustophoretic patterning, removing particles from assembly zones is achieved by applying an intermediary acoustic wave.

We experimentally demonstrate our approach using polystyrene microspheres in planar psuedo-standing waves generated with a single-transducer setup. Our patterning device is built around a 10 mm $\times$ 50 mm $\times$ 45 mm fluorescence glass cuvette (Figure 1). Acoustic waves are generated by a 25 mm diameter, 500 kHz broadband transducer driven by a signal generator and power amplifier. To ensure good acoustic contact throughout the patterning process, the transducer was mounted to the cuvette with ultrasonic couplant and clamped into place. Polystyrene microspheres with diameters of 98 ± 1.5 μm (standard deviation) served as the particles for patterning and were suspended in a solution of 75% deionized water and 25% glycerol to make the microspheres neutrally buoyant. The glycerol-water solution is commonly used in fluid experiments and has been well characterized[31]. A small magnetic stir bar was added to the cuvette to allow the microspheres to be remixed after patterning to re-set the device for subsequent experiments. During patterning, the magnetic stir bar was held in a corner of the cuvette with a small magnet. A marking strip was mounted to the cuvette to orient the camera field of view and ensure the camera remained focused on the same region of interest within the cuvette throughout the experiments.

The setup we use is similar to those of other studies and can be suitably modeled with planar standing waves[11], which is also consistent with our observed microsphere patterns. The primary ARF from a plane standing wave with wavenumber, k, on a sphere with radius, a, such that $ka \ll 1$ is[34]:

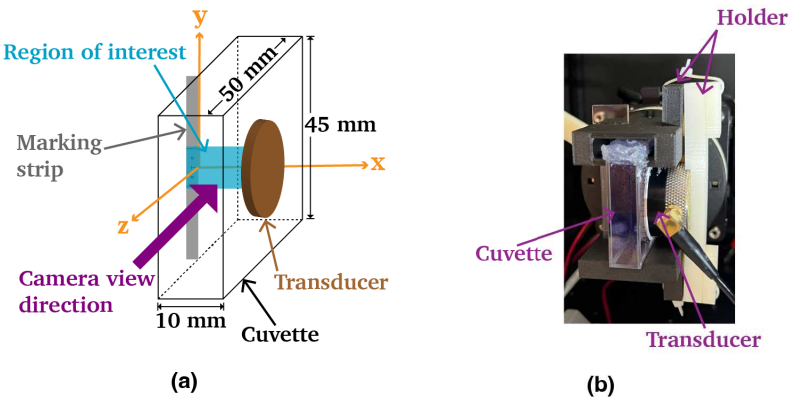

FIG. 1. (a) Schematic of the cuvette and the coordinate system. The origin is set at the inner side of the left cuvette wall and the **x**-axis goes through the center of the transducer. The camera views the cuvette along the **z**-axis and is focused on the region of interest, shown in blue. The marking strip was used to identify the region of interest in the camera frame. *Adapted with permission from Y. J. Wang. Formation Process of Acoustophoretic Patterns. PhD thesis, Massachusetts Institute of Technology, 2022.* (b) A holder was used to attach the transducer to the cuvette to maintain good acoustic contact. Ultrasonic couplant was applied between the transducer and the cuvette.

$$\mathscr{F}_{ARF} = \frac{\pi}{3}\rho_f |A|^2 (ka)^3 R \sin(2kx)\hat{x} \tag{1}$$

$$R = \frac{5\rho_s - 2\rho_f}{2\rho_s + \rho_f} - \frac{\rho_f c_f^2}{\rho_s c_s^2} \tag{2}$$

where $|A|$ is the amplitude of the velocity potential of the wave; $\hat{x}$ is the unit vector in the **x** direction; ρ is fluid density; c is the speed of sound; and the subscripts f and s indicate properties of the fluid and sphere, respectively. x is the location of the sphere with $x = 0$ corresponding to a pressure antinode. Using the rigid wall boundary condition, the normal velocity of the fluid is 0 at the walls of the cuvette, making the cuvette walls pressure antinodes. Thus, we set $x = 0$ at the inner edge of the left side of the cuvette. As shown in Figure 2, the ARF acts along the **x**-axis. It is constant with respect to time, but varies sinusoidally over space, completing a full cycle over the distance of $\lambda/2$. Depending on the sign of R, the particles will travel towards the pressure nodes or antinodes, where $\mathscr{F}_{ARF} = 0$. When $R > 0$, the antinodes are unstable equilibrium locations while the pressure nodes are stable, and vice versa when $R < 0$. In this work, the density of the fluid was

matched to that of the polystyrene microspheres so R can be simplified to:

$$R = 1 - \left(\frac{c_f}{c_s}\right)^2 \tag{3}$$

The speed of sound of our glycerol-water solution is 1630 m/s and the speed of sound of polystyrene is 2350 m/s[8]. Therefore, $R > 0$ for our setup, and the polystyrene microspheres collect at the pressure nodes.

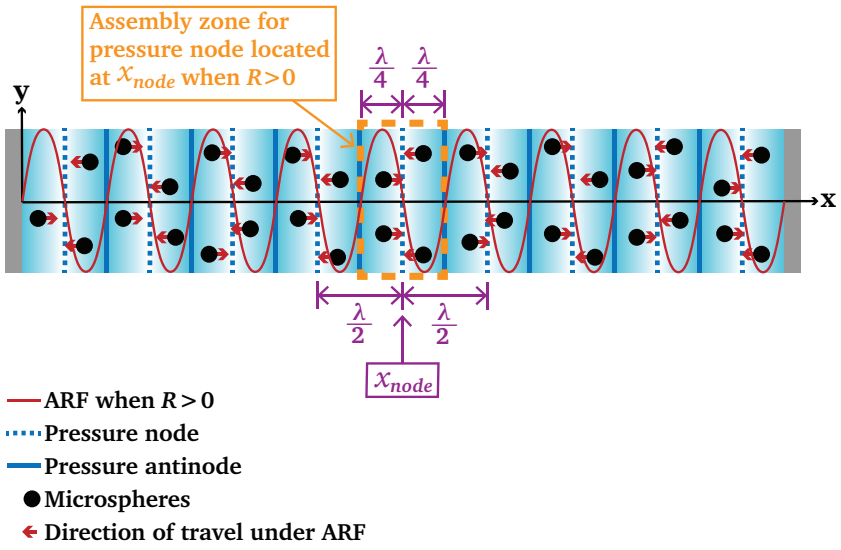

FIG. 2. The acoustic radiation force in a plane standing wave is spatially sinusoidal. When $R > 0$, the microspheres move towards their closest pressure nodes, and only microspheres within the assembly zone of a pressure node will be driven toward that pressure node. The assembly zone of the pressure node located at x_{node} is the region from $x_{node} - \lambda/4$ to $x_{node} + \lambda/4$. Evacuating microspheres from this assembly zone prior to applying the acoustic wave would leave this pressure node empty in the acoustophoretic pattern. *Adapted with permission from Y. J. Wang. Formation Process of Acoustophoretic Patterns. PhD thesis, Massachusetts Institute of Technology, 2022.*

The acoustic wave determines the spatial variation of the ARF, which in turn determines the pattern geometry. Thus, existing methods for acoustophoretic patterning typically focus on creating waves with novel pressure node and antinode positions. Our method relies on using one acoustic wave to evacuate some assembly zones of the subsequent wave. The assembly zone of each stable equilibrium location is determined by the location of the other equilibrium locations.

For the materials used in this work $R > 0$, so we primarily focus on the pressure nodes as the stable equilibrium locations for the rest of this work. Multiple pseudo-plane standing wave modes can be excited inside the cuvette by driving the transducer at different frequencies, which we model as a 1D wave with length, L. Using the rigid wall boundary condition, the normal velocity of the fluid is 0 at the walls of the cuvette, making the cuvette walls pressure antinodes. The first mode will contain 1 pressure node, the second mode will contain 2 pressure nodes, and so on. In general, the Nth resonant mode contains N pressure nodes and has a wavelength of

$$\lambda_N = \frac{2L}{N} \tag{4}$$

and frequency

$$f_N = \frac{Nc_f}{2L} \tag{5}$$

The nth node from the left is located at

$$x_{N:n} = \frac{\lambda_N}{2}\left(n - \frac{1}{2}\right) \tag{6}$$

where $x = 0$ is the distance from the left fluid boundary. For clarity, pressure nodes in this work will be labeled N:n to distinguish between the individual pressure nodes in the different standing wave modes.

For the 1D plane standing wave, the assembly region extends from $\lambda/4$ to the left of the equilibrium location to $\lambda/4$ to the right of the equilibrium (Figure 2). The assembly zone associated with each node is

$$x_{N:n} - \frac{\lambda_N}{4} < x < x_{N:n} + \frac{\lambda_N}{4} \tag{7}$$

$$\frac{\lambda_N}{2}(n-1) < x < \frac{\lambda_N}{2}n \tag{8}$$

Evacuating microspheres from the assembly zone prior to applying the wave will leave the associated pressure node empty in the microsphere pattern. Leaving pressure nodes empty creates non-uniform spacing between the microsphere bands. We demonstrate using an intermediary acoustic wave to evacuate assembly zones.

As a proof of concept of our method, we use $N = 6$ as the intermediary wave and $N = 9$ as

the final wave. For our experimental setup, we selected 489 kHz for the $N = 6$ wave and 734 kHz for the $N = 9$ wave by first estimating the frequency from the fluid properties and cuvette length using Equation 5. Then, multiple banding trials were conduced at frequencies around the estimate to fine-tune the quality of the bands. The microspheres were remixed between each trial. The selected frequencies gave sharp, straight bands, and the band locations agreed well with the predicted pressure node locations from Equation 6 (Figure 3).

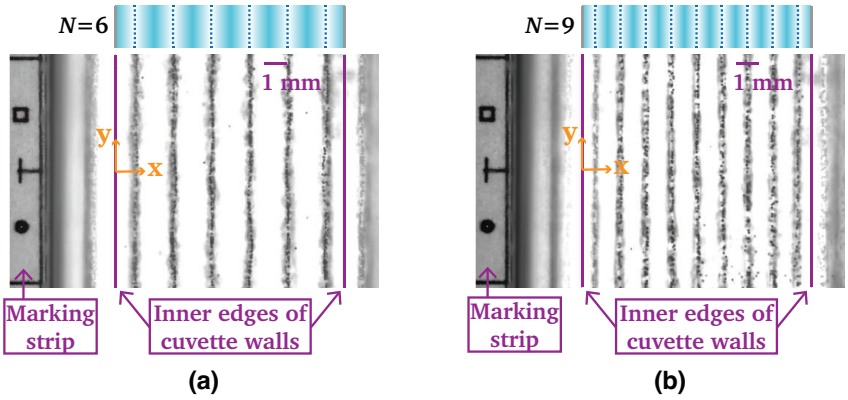

FIG. 3. Observed banding patterns for the (a) $N = 6$ and (b) $N = 9$ waves within the region of interest indicated in Figure 1b. The edges of the cuvette were determined using the marking strip because the clear glass cuvette walls do not show up distinctly on camera. For reference, the schematic of the expected pressure nodes are shown above each experimental image. The observed microsphere pattern inside the cuvette is consistent with plane standing waves and the location of the bands are consistent with the expected pressure node locations. *Adapted with permission from Y. J. Wang. Formation Process of Acoustophoretic Patterns. PhD thesis, Massachusetts Institute of Technology, 2022.*

Equation 8 predicts that patterning at $N = 6$ will move the microspheres out of the assembly zones of pressure nodes 9:2, 9:5, and 9:8 so that these three locations will be empty in the final pattern. To experimentally verify this prediction, the transducer was first driven at 489 kHz for 15 s to form the $N = 6$ pattern. Then, the driving frequency was switched to 734 kHz for 20 s to create the final pattern. During the switch, the microsphere pattern created by the 489 kHz wave remained stable and microspheres were not observed to re-enter the assembly zones of pressure nodes 9:2, 9:5, and 9:8. As expected, the pressure nodes 9-2, 9-5, and 9-8 are left empty in the final pattern. This results in a final pattern with 6 bands with spacing between the bands varying between 1.1 mm and 2.2 mm. A schematic and experimental images of this multi-step patterning

process are shown in Figure 4.

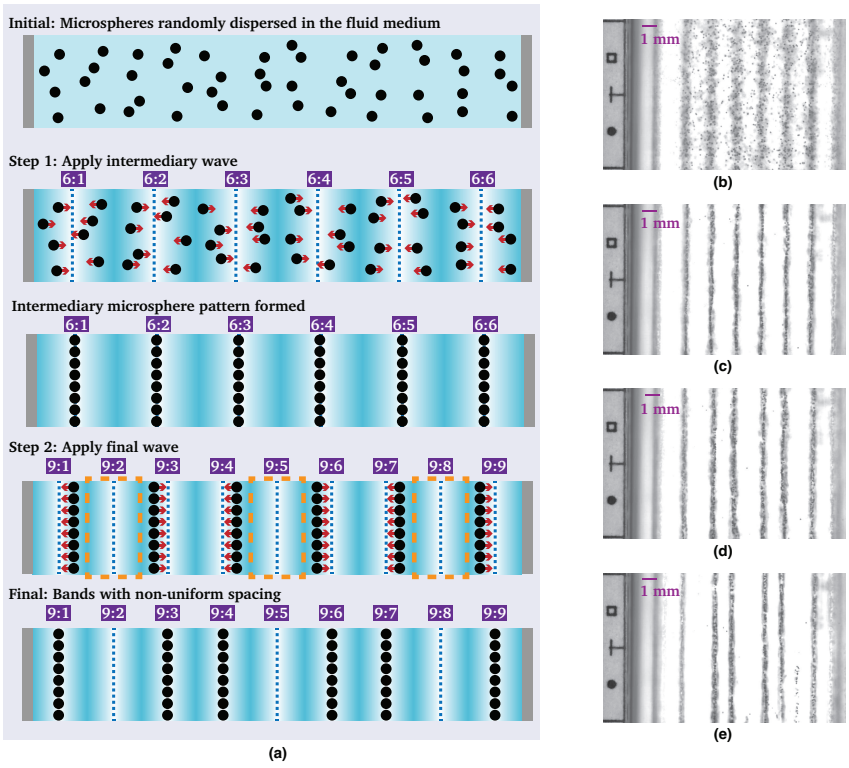

FIG. 4. The process of applying two frequencies in sequence to create acoustophoretic patterns with non-uniform spacing between microsphere bands. (a) Schematic of the patterning process. The microspheres are initially randomly dispersed in the fluid medium. Step 1: apply the intermediary wave to move the microspheres out of assembly zones in the final wave. In this demonstration, $R > 0$ and we use the wave $N = 6$ to drive the microspheres to the 6 pressure nodes. Step 2: apply the final wave. In our example, we use the wave $N = 9$. All 6 bands formed in step 1 are outside the banding zones of 9:2, 9:5, and 9:8 so these nodes will not contain microspheres in our final pattern. *Adapted with permission from Y. J. Wang. Formation Process of Acoustophoretic Patterns. PhD thesis, Massachusetts Institute of Technology, 2022.* (b) Experimental image of the $N = 6$ pattern being formed. (c) Pattern before the transducer driving frequency is switched. (d) Switching to the $N = 9$ wave drives the formed bands to new locations. (e) Final acoustophoretic pattern with non-equal spacing between bands.

The model we use for predicting the pattern formed by sequencing waves include some key limitations. We note that Equation 1 considers the interaction between the wave and a single microsphere and does not consider effects from neighboring particles. It is also possible that

secondary effects and other effects from the formed pattern may cause subsequent waves to deviate from the expected primary ARF patterning behavior. However, in this work, the existence of the formed bands do not significantly disrupt the patterning. Additionally, in our simplified model, the assembly zones around each equilibrium location have sharp edges located exactly mid-way to the next equilibrium location. Under experimental conditions, the precise location of the boundaries may be challenging to predict and control so a margin of error may be required when designing the wave sequences to guarantee that an equilibrium location is empty in the final pattern. More work is needed to understand the impacts of these simplifications on what type of patterns can be created by applying waves in sequence.

Applying an intermediary wave allows certain equilibrium locations to be left empty in the final particle pattern. Thus, the types of pattern geometries that can be created by sequencing acoustic waves are inherently limited by how many times the wave can be switched and which waves can be generated within the device. When the acoustic wave is switched, it takes time for the particles to move to new positions so the number of switches is limited by the total amount of time available for forming the particle pattern. The time for forming the particle pattern may be limited by output requirements for specific applications and by physics effects that disrupt the patterning over time, such as acoustic streaming and settling when particles cannot be made neutrally buoyant. Additional work is required to fully understand the limitations on how many acoustic wave can be applied in sequence. The pattern geometries that can be created by sequencing different acoustic waves is also limited by which acoustic waves can be generated within the device. In single-transducer setups, the bandwidth of the transducer limits which acoustic resonant modes can be activated. Therefore, transducers with low Q-factors and a large bandwidth would be beneficial for reaching more resonant modes. However, the low Q-factor also makes the setup less energy efficient[10], which is also an important consideration when scaling up acoustophoretic patterning in applications. It may also be possible to apply our technique to setups with more than one transducer, which would provide a way to balance between the need to control the particle pattern geometry with the constraints on incorporating additional transducers into the setup.

Although we limited our demonstration to two pseudo-plane standing waves, the method of applying multiple waves in sequence during acoustophoretic patterning may be applicable to other wave geometries and additional waves in the sequence. Resonant cavities with different resonant wave geometries depending on where it is excited, such as ovals, could be particularly interesting

for patterning using a sequence of resonant modes. The sequencing method can also be used in conjunction with other wave forming techniques to give further control over where the particles collect to produce higher quality final patterns. Applying multiple acoustic waves sequentially during acoustophoretic patterning expands the design parameters available to engineers and presents a method to increase achievable pattern geometries without increasing hardware complexity, which could simplify incorporating acoustophoretic patterning into manufacturing processes.

In summary, this work has demonstrated an alternate approach for creating more complex geometries in acoustophoretic patterning. Instead of increasing hardware complexity to create more complex wave geometries, we increased the number of simple wave geometries used in the patterning process. We demonstrated our approach by using two pseudo plane standing waves to achieve an acoustophoretic pattern with unequal spacing between bands, a pattern geometry that would not be achievable by using only a single pseudo plane standing wave. More work is still required to fully develop sequencing waves as a method of creating acoustophoretic patterns, such as further understanding the impact of a formed pattern on the acoustic wave. By introducing a different approach to use in acoustophoretic patterning design, our method could allow more geometries to be achievable in settings where hardware complexity is a constraint.

I. AUTHOR DECLARATIONS

Portions of this letter previously appeared in a Ph.D. thesis[32]. Reproduced with permission from MIT.

The data that support the findings of this study are available from the corresponding author upon reasonable request.

REFERENCES

[1]S. Burgarella, S. Merlo, B. Dell'Anna, G. Zarola, and M. Bianchessi. A modular micro-fluidic platform for cells handling by dielectrophoresis. *Microelectron. Eng.*, 2010.

[2]L. A. Chai and B. W. Anthony. Organization and compaction of composite filler material using acoustic focusing. In *Proc. IMECE*. ASME, 2017.

[3]E. Cherkaev, F. G. Vasquez, C. Mauck, M. Prisbrey, and B. Raeymaekers. Wave-driven assembly of quasiperiodic patterns of particles. *Phys. Rev. Lett.*, 2021.

[4]M.-Y. Chiang, Y.-W. Hsu, H.-Y. Hsieh, S.-Y. Chen, and S.-K. Fan. Constructing 3d heterogeneous hydrogels from electrically manipulated prepolymer droplets and crosslinked microgels. *Sci. Adv.*, 2016.

[5]S. Cohen, H. Sazan, A. Kenigsberg, H. Schori, S. Piperno, H. Shpaisman, and O. Shefi. Large-scale acoustic-driven neuronal patterning and directed outgrowth. *Sci. Rep.*, 2020.

[6]L. Cox, K. Melde, A. Croxford, P. Fischer, and B. W. Drinkwater. Acoustic hologram enhanced phased arrays for ultrasonic particle manipulation. *Phys. Rev. Applied*, 2019.

[7]N. B. Crane, O. Onen, J. Carballo, Q. Ni, and R. Guldiken. Fluidic assembly at the microscale: progress and prospects. *Microfluid. Nanofluidics*, 2013.

[8]CRC. *CRC handbook of chemistry and physics.*, Speed of sound in various media. CRC Press, Cleveland, Ohio, 2022.

[9]B. W. Drinkwater. Dynamic-field devices for the ultrasonic manipulation of microparticles. *Lab Chip*, 2016.

[10]J. Dual, P. Hahn, I. Leibacher, D. Möller, and T. Schwarz. Acoustofluidics 6: Experimental characterization of ultrasonic particle manipulation devices. *Lab Chip*, 2012.

[11]P. Glynne-Jones, R. J. Boltryk, and M. Hill. Acoustofluidics 9: Modelling and applications of planar resonant devices for acoustic particle manipulation. *Lab Chip*, 2012.

[12]P. Glynne-Jones, C. E.M. Demore, C. Ye, Y. Qiu, S. Cochran, and M. Hill. Array-controlled ultrasonic manipulation of particles in planar acoustic resonator. *IEEE Trans. Ultrason. Ferroelectr. Freq. Control*, 2012.

[13]J. Greenhall, F. G. Vasquez, and B. Raeymaekers. Ultrasound directed self-assembly of user-specified patterns of nanoparticles dispersed in a fluid medium. *Appl. Phys. Lett.*, 2016.

[14]B. A. Grzybowski, C. E. Wilmer, J. Kim, K. P. Browne, and K. J. M. Bishop. Self-assembly: from crystals to cells. *Soft Matter*, 2009.

[15]F. G. Vasquez and C. Mauck. Periodic particle arrangements using standing acoustic waves. *Proc. R. Soc. A: Math. Phys. Eng. Sci.*, 2019.

[16]B. Kang, J. Shin, H.-J. Park, C. Rhyou, D. Kang, S.-J. Lee, Y.-S. Yoon, S.-W. Cho, and Hy. Lee. High-resolution acoustophoretic 3d cell patterning to construct functional collateral cylindroids for ischemia therapy. *Nat. Commun*, 2018.

[17]K. Kolesnik, M. Xu, P. V. S. Lee, V. Rajagopal, and D. J. Collins. Unconventional acoustic approaches for localized and designed micromanipulation. *Lab Chip*, 2021.

[18]X. Li, K. M. Lim, and W. Zhai. A novel class of bioinspired composite via ultrasound-assisted directed self-assembly digital light 3d printing. *Appl. Mater. Today*, 2022.

[19]T. M. Llewellyn-Jones, B. W. Drinkwater, and R. S. Trask. 3d printed components with ultrasonically arranged microscale structure. *Smart Mater. Struct.*, 2016.

[20]E. MacDonald and R. Wicker. Multiprocess 3d printing for increasing component functionality. *Science*, 2016.

[21]M Mastrangeli, S Abbasi, C Varel, C Van Hoof, J-P Celis, and K F Böhringer. Self-assembly from milli- to nanoscales: methods and applications. *J. Micromech. Microeng.*, 2009.

[22]K. Melde, E. Choi, Z. Wu, S. Palagi, T. Qiu, and P. Fischer. Acoustic fabrication via the assembly and fusion of particles. *Adv. Mater.*, 2018.

[23]K. Melde, A. G. Mark, T. Qiu, and P. Fischer. Holograms for acoustics. *Nature*, 2016.

[24]G. C. Pidcock and M. in het Panhuis. Extrusion printing of flexible electrically conducting carbon nanotube networks. *Adv. Funct. Mater.*, 2012.

[25]M. Prisbrey, J. Greenhall, F. Guevara Vasquez, and B. Raeymaekers. Ultrasound directed self-assembly of three-dimensional user-specified patterns of particles in a fluid medium. *J. Appl. Phys.*, 2017.

[26]J. H. E. Promislow and A. P. Gast. Magnetorheological fluid structure in a pulsed magnetic field. *Langmuir*, 1996.

[27]B. Raeymaekers, C. Pantea, and D. N. Sinha. Manipulation of diamond nanoparticles using bulk acoustic waves. *J. Appl. Phys.*, 109(1):014317, Jan 2011.

[28]M.-S. Scholz, B. W. Drinkwater, T. M. Llewellyn-Jones, and R. S. Trask. Counterpropagating wave acoustic particle manipulation device for the effective manufacture of composite materials. *IEEE Trans. Ultrason*, 2015.

[29]S. Shet, V. R. Mehta, A. T. Fiory, N. M. Ravindra, and M. P. Lepselter. The magnetic field-assisted assembly of nanoscale semiconductor devices: A new technique. *JOM*, 2004.

[30]K.-W. Tung and P.-Y. Chiou. Field-programmable acoustic array for patterning micro-objects. *Appl. Phys. Lett.*, 2020.

[31]A. Volk and C. J. Kähler. Density model for aqueous glycerol solutions. *Exp. Fluids*, 2018.

[32]Y. J. Wang. *Formation Process of Acoustophoretic Patterns*. PhD thesis, Massachusetts Institute of Technology, 2022.

[33]G. M. Whitesides and M. Boncheva. Beyond molecules: self-assembly of mesoscopic and

macroscopic components. *Proc. Natl. Acad. Sci. U. S. A.*, 2002.

[34]K. Yosioka and Y. Kawasima. Acoustic radiation pressure on a compressible sphere. *Acustica*, 1955.

[35]D. E. Yunus, S. Sohrabi, R. He, W. Shi, and Y. Liu. Acoustic patterning for 3d embedded electrically conductive wire in stereolithography. *J. Micromech. Microeng*, 2017.

PLEASE CITE THIS ARTICLE AS DOI: 10.1063/5.0112113

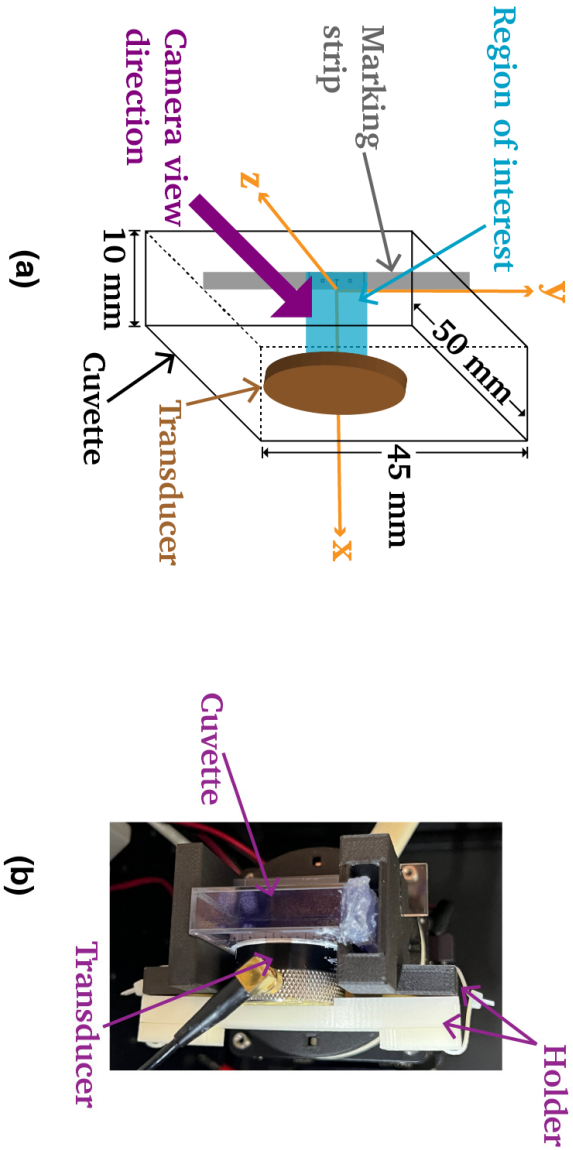

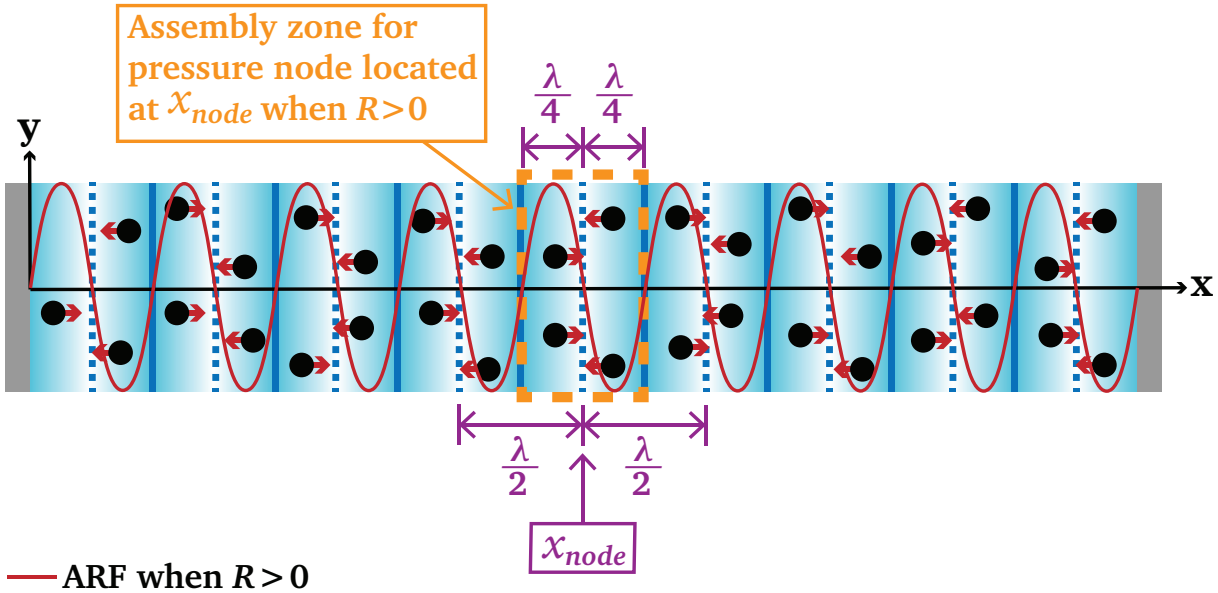

PLEASE CITE THIS ARTICLE AS DOI: 10.1063/5.0112113